Light-Induced Electron Transfer in Pyropheophytin−Anthraquinone Dyads: Vectorial Charge Transfer in Langmuir−Blodgett Films

N. V. Tkachenko,*,† A. Y. Tauber,†,‡ P. H. Hynninen,‡ A. Y. Sharonov,§ and H. Lemmetyinen†

Institute of Materials Chemistry, Tampere University of Technology, P.O. Box 541, FIN-33101, Tampere, Finland, Department of Chemistry, University of Helsinki, P.O. Box 55, FIN-00014, Helsinki, Finland, and General Physics Institute of Russian Academy of Science, Vavilov str. 38, Moscow, Russia

Received: September 17, 1998; In Final Form: January 20, 1999

Novel types of donor−acceptor (DA) compounds, consisting of covalently linked pyropheophytin−anthraquinone molecules (PQ1 and PQ2) and their Zn derivatives (ZnPQ1 and ZnPQ2) have been previously synthesized and studied in a variety of solvents. The compounds are retaining the chlorophyll phytyl tail, which makes them suitable for the Langmuir−Blodgett (LB) technique. The technique enables one to prepare solid films capable of performing vectorial intramolecular light-induced electron transfer (ET). The DA compounds form stable monolayers on a water surface and the monolayers can be transferred onto a solid substrate. The ET properties of the LB films were tested by means of time-resolved fluorescence spectroscopy and direct transient photovoltaics measurements. In 100% films, an intramolecular ET is strongly reduced as a result of intermolecular aggregation between the DA molecules. To prevent the aggregation, the DA compounds were placed in a matrix of soft lipids (e.g., lipids with unsaturated carbon chains) and methods to achieve uniform deposition of multilayer films were developed. The highest efficiency of the intramolecular ET was obtained for the multilayer films prepared by combining layers of ZnPQ1 in a Soya lipids matrix with dipalmitoylphosphatidic acid as the bottom and intermediate layers. The sign of the signals in the photovoltaics measurements and, therefore, the direction of the ET can be controlled by the deposition direction of the DA active layers.

1. Introduction

The design of molecular systems capable of performing light-induced charge separation (CS) has been a subject of intensive studies during the last few decades.[1,2] A variety of donor−acceptor (DA) compounds have been synthesized and studied. To utilize the microscopic intramolecular CS in macroscopic dimensions, the DA molecules have to be ordered uniformly in one direction to establish a vectorial charge transfer in the sample. One of the useful techniques for building up highly ordered molecular systems is the Langmuir−Blodgett (LB) method.[3−21] The application of this method to DA compounds imposes certain requirements on the structure and, hence, synthesis of the compounds. The molecules must be insoluble in water in order to form a monolayer on the water surface and to keep them orientated on the surface. The desired goal is usually achieved by a proper combination of hydrophilic and hydrophobic groups in the DA molecules.

Recently, four covalently linked pyropheophytin−anthraquinone compounds have been synthesized.[22,23] In addition to a donor−bridge−acceptor system, these compounds are retaining the chlorophyll phytyl tail, which makes them suitable for the LB technique.[8] The photochemical properties of the DA compounds have been studied in a variety of solvents, and a fast light-induced ET has been observed.[24] These compounds can form monolayers on the water surface by themselves or, alternatively, they can be incorporated into a layer of lipid molecules. A preliminary study of one of the DA dyads has shown light-induced ET in monolayers of dioleylphosphatidylcholine.[8]

In the present study, four DA compounds were investigated using a variety of lipid matrixes in monolayer and multilayer films. Our goal was to optimize the vectorial photoinduced electron transfer (PET) function of the solid LB films. Two measuring methods were employed in order to characterize the ET properties of the films. The first method is the measurement of steady-state and time-resolved fluorescence and the second one is the transient photoelectric technique. The fluorescence method enables one to follow the singlet excited-state kinetics. That is a powerful but an indirect method, since the lifetime of the excited state may be affected by factors other than the ET process.

One of the undesirable phenomena is the aggregation of chromophores in LB films.[5−7,16] Fortunately, there are methods to distinguish between the fluorescence quenchings arising from the ET and the aggregation. The ET results in a reduction of the fluorescence lifetime, while the fluorescence spectrum remains essentially undisturbed. The aggregation might also lead to a reduction in the lifetime, but most aggregates have a fluorescence spectrum different from that of the monomer.

The transient photoelectric[9−11,21] technique was developed to investigate a fast light-induced motion of charges in LB films. It is based on measurements of the light-induced Maxwell displacement charge and it enables one to study the charge shift in the direction perpendicular to the film plane. In comparison to the well-known photocurrent measurements developed for photochemical cells,[12,13,17−19] this method provides a higher time

† Tampere University of Technology.
‡ University of Helsinki.
§ Russian Academy of Science.

10.1021/jp983766i CCC: $18.00
Published on Web 04/22/1999

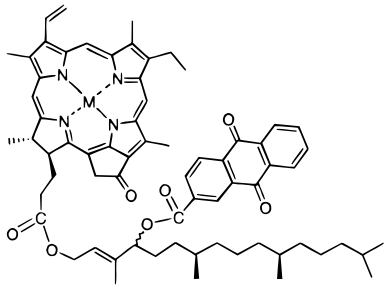

PQ1, PQ2 (M = 2H) and **ZnPQ1, ZnPQ2** (M = Zn)

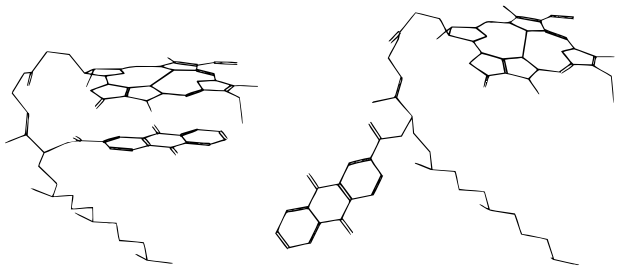

a) folded conformer b) open conformer

Figure 1. Chemical structure of PQ1 and PQ2 and its two main conformers.

resolution (20 ns at present) and does not need the charge transport through the sample. Thus, one can study the formation and recombination of the intramolecular CS state. To apply this technique, all of the DA molecules should have the same orientation. This situation can be achieved in the case of LB films by depositing the active DA layers in one direction. The films are placed between two electrodes, and the DA layers are insulated from both of the electrodes to avoid direct interaction of the DA molecules with the conductors (or semiconductors). The films for electric measurements are multilayer structures: (electrode)/insulating layers/DA layer(s)/insulating layers/(electrode). Methods of smooth multilayer deposition are of great importance for this investigation technique.

This study was divided into several steps. In the first step, the monolayer films were studied. The ET properties were tested by time-resolved fluorescence spectroscopy. On the basis of this knowledge, the methods for the preparation of ordered multilayer films were developed. Comparison of the fluorescence properties of the monolayer and multilayer films gave information about the DA molecule functioning. Finally, multilayer films were prepared on the indium−tin oxide (ITO) electrodes and their photoelectric responses were recorded. This method provides direct information about the light-induced charge motion in the direction perpendicular to the film plane. The optimization of the film structure in order to obtain the highest intensity of the photoelectric response is the objective of the present work.

2. Methods and Materials

2.1. Materials. The synthesis and complete chromatographic separation of the P4 diastereomers of 13^2-demethoxycarbonyl-P4-oxy-(9,10-anthraquinone-2-carbonyl)−pheophytin *a* (PQ1 and PQ2, Figure 1) were accomplished as reported earlier.[23] The zinc(II) insertion into PQ1 and PQ2 and the reference compounds was carried out according to the published procedure.[8] The metalation resulted quantitatively in the Zn(II) complexes of the pyropheophytin−anthraquinone dyads (ZnPQ1 and ZnPQ2, Figure 1).

Six lipids were used as the matrixes for the DA compounds: dioleoyl *L*-α-phosphatidylcholine (DOPC, Sigma), Soya PC, erucic acid (EA, Aldrich), stearic acid (SA, Sigma), stearylamine (SAm, Sigma), and dipalmitoyl *L*-α-phosphatidic acid (DPPA, Sigma). All lipids were of at least 99% grade and were used as purchased. The subphases for the films were 0.1 mM $CdCl_2$ for the SA and alternate films, 0.3 mM phosphate buffer (pH = 7) for DOPC and SAm, and 0.1 mM $CaCl_2$ for DPPA. The water for the subphase preparation was purified using a Milli-Q system (Millipore).

2.2. LB Films. The LB films were prepared using single- or double-trough instruments (LB 2000 or LB 5000 Alt of KSV Instruments, Helsinki, Finland). Quartz plates (35 × 12 × 1 mm) were used to deposit the films for fluorescence studies. In the photoelectric measurements, quartz plates coated with an ITO semitransparent thin electrode were used. The plates were cleaned before the film deposition using the standard procedure.[4]

2.3. Time-Resolved Fluorescence Measurements. The setup for the time-resolved fluorescence measurements is described elsewhere.[6] Briefly, it consisted of a picosecond dye laser synchronously pumped by a mode-locked Nd^{2+} YAG laser (Series 3000, Spectra-Physics). The excitation wavelength was 590 nm, the pulse duration 20 ps, and the pulse repetition rate 800 kHz. The registration consisted of a time-correlated single-photon counting instrument (model 199, Edinburgh Instrument) equipped with a microchannel plate photomultiplier (Hamamatsu R2809-50). The instrumental response time was approximately 120 ps.

2.4. Time-Resolved Photoelectric Measurements. The setup for the time-resolved photoelectric measurements is described in detail elsewhere.[9−11,21] In short, a dye laser pumped by an excimer laser was used for the excitation, the pulse duration was ∼30 ns and the wavelength was 430 nm (Coumarine 120 dye). The films were placed into a metal shielding box incorporating two preamplifiers. One preamplifier with an input resistance of 10^{10} Ω (typical value) and a bandwidth from dc to 1 MHz was used for micro- to millisecond time scale measurements. Another amplifier with an input resistance of 100 kΩ and a bandwidth from 0.01 to 50 MHz was used for nanosecond time scale measurements. Amplified signals were digitized by Tektronix 7912AD or 2212 and averaged (typically 20−60 curves) by a PC, controlling the experiments. An external dc voltage from −1.2 to +1.2 V can be applied to the sample in order to study the influence of the electric field on the photoelectric response. The conductance and capacitance of the sample were always checked before and after measurements.

In the photoelectric measurements, the film can be treated as a flat capacitor. One electrode of the capacitor is the ITO layer, which is also a support for the deposited LB film. Another electrode is a drop of an InGa alloy, gently attached to the film. The functional DA layers were always insulated from the electrodes to avoid any interaction of the DA compounds with the conductors. Typically nine insulating layers of SAm or DPPA were deposited directly onto the ITO electrode prior to deposition of the DA layers. Finally, the DA layers were covered by 10 insulating layers of SAm or DPPA. Based on our previous experience,[9] this can ensure that no direct contact of the DA compounds with the electrodes takes place. Ideally, the film samples can be considered as a pure insulators. Thus, there was no steady-state current across the sample when a bias voltage was applied. The measured Maxwell displacement charge was created by the motion of charges induced by the light in the DA layers. The charge, however, did not reach the electrodes.

It is possible to manufacture film samples with two complementary structures capable of performing vectorial PET. The

first type of structure was prepared by depositing the DA layers upstroke and the supporting layers downstroke. Schematically, the samples can be drawn as follows:

```
     |>-- --< DA- --< DA- --< >--  /
     |>-- --< >~~ --< >~~ --< >-- |
     |>-- --< DA- --< DA- --< >-- |
ITO  |>-- --< >~~ --< >~~ --< >-- | top electrode
     |>-- --< DA- --< DA- --< >-- |
     |>-- --< >~~ --< >~~ --< >-- |
     |>-- --< DA- --< DA- --< >--  \
```

Here, - -< denotes insulating molecules, >∼∼ is the matrix molecule for the DA compound, and DA− is the DA compound. The second structure was deposited in the opposite direction:

```
     |>-- --< >-- -AD >-- -AD >--  /
     |>-- --< >-- ~~< >-- ~~< >-- |
     |>-- --< >-- -AD >-- -AD >-- |
ITO  |>-- --< >-- ~~< >-- ~~< >-- | top electrode
     |>-- --< >-- -AD >-- -AD >-- |
     |>-- --< >-- ~~< >-- ~~< >-- |
     |>-- --< >-- -AD >-- -AD >--  \
```

In the ideal case structures **1** and **2** should produce photoelectric signals that are similar in amplitude but of different polarities. This kind of photoresponse is direct evidence for the sample structure and for the vectorial charge transfer.

Another evidence of the DA molecules arrangement in the layer is whether an external static electric field has an influence on the photoelectric signal. Two extreme situations are represented by the transient photoelectric responses obtained from the 100% chlorophyll *a* (Chl) films[11] and from the films containing the electrostatic porphyrin−phthalocyanine DA heterodimers.[21] In the first case, the photoresponse signal is determined by the photoinduced charge migration in the Chl self-aggregates and the polarity and intensity of the signal are fully controlled by the applied external electric field. In the second case, the polarity of the signal is determined by the orientation of the DA heterodimer and the driving force for creation of the Maxwell displacement charge is the orientation of the DA heterodimer in respect to the electrodes.

3. Results and Discussions

The DA compounds have been intensively studied by means of NMR[22,25] and by steady-state and time-resolved absorption and fluorescence spectroscopies in different solvents.[24] The preliminary results from the fluorescence investigations of the ZnPQ1 monolayers in the DOPC matrix have also been reported.[8] On the basis of these studies, one can expect two main types of conformers of the DA compounds to be present in the films. The first one is a folded conformer with the shortest donor−acceptor distance of approximately 4 Å for the Zn compounds and 6−8 Å for the metal-free compounds. This is the dominating type of conformer. Another type of conformer has a noticeably longer separation between the donor and acceptor (estimated value is 15−20 Å). Its relative amount depends on the DA compound and the environment and was estimated to vary between 5 and 30%. The folded conformers of the Zn compounds undergo fast light-induced ET in less than a few picoseconds in solutions of different polarity, such as toluene, acetone, or methanol. The metal-free DA compounds (PQ1,2) perform ET in solvents of moderate or high polarity (the ET rate constant in acetonitrile is close to 10^{12} s^{-1}). The folded conformer is supposed to dominate in LB films as it has a more compact arrangement and, therefore, may be favored thermodynamically.

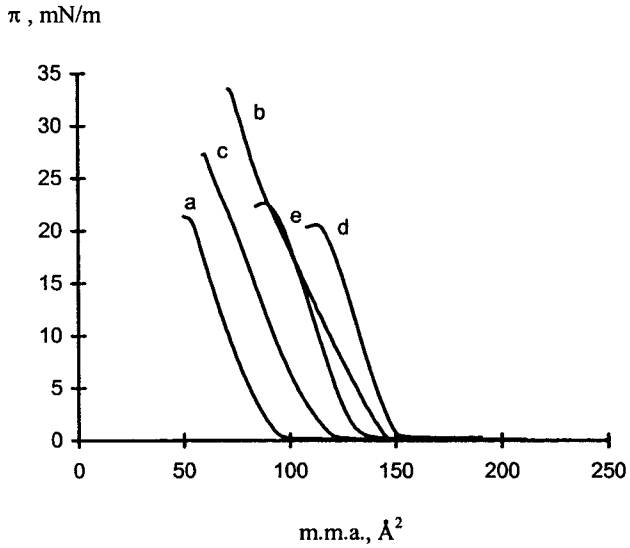

Figure 2. Surface pressure isotherms of (a) ZnP, (b) ZnPQ1, (c) ZnPQ2, (d) PQ1, and (e) PQ2 on a pure water subphase.

3.1. Films of the Pure DA Compounds. Each of the four DA compounds forms a monolayer on the water surface, exhibiting reasonable mean molecular area (mma). The surface pressure isotherms (π vs mma) were recorded on a pure water subphase for all of the compounds. The resulting isotherms for PQ1, PQ2, ZnPQ1, ZnPQ2, and for the quinone-free reference compound (ZnP) are shown in Figure 2. From these results, three conclusions can be drawn.

(1) For the Zn compounds, the areas are smaller than those for the metal-free derivatives.

(2) The P4 R stereoisomers have higher mma values than the P4 S stereoisomers (e.g., PQ1 vs PQ2).

(3) The metal-free compounds have lower collapse pressures than the corresponding Zn compounds.

The first conclusion is in agreement with the molecular structure models, showing that the center-to-center distance between the donor and acceptor for the Zn compounds is shorter than that for the metal-free compounds. This suggests that the Zn compounds may have a more compact conformation, resulting in a denser packing in the monolayer. The P4 diastereomers have about the same DA center-to-center distance, but the orientations of the phorbin and quinone rings are different. In addition, the conformations of the phytyl groups are completely different for the diastereomers, which results in a distinct difference in the relative mma for the diastereomers (Figure 2). The tighter packing may provide a more stable layer and results in a higher collapse pressure for the Zn derivatives.

Monolayers of the pure DA compounds can be deposited on a solid support. There is evidence that porphyrins[7] and chlorophyll *a*[5,6,16] form aggregates in the 100% LB films. This aggregation is usually characterized by a broadening of the absorption bands, a red-shift and a broadening of the emission bands and a gradual decrease in the lifetime of the singlet excited state.[5−7,16] Similar phenomena have been observed for the DA compounds in the LB films now under investigation. The fluorescence spectra of the film samples were significantly red-shifted. The fluorescence intensities were low and the fluorescence decay profiles were short with the shape close to the instrumental response function, indicating lifetimes shorter than 100 ps.

The film samples for the electric measurements were prepared for all pure DA compounds (pairs of samples with structures **1** and **2** were made in all cases). For PQ1 and PQ2, the

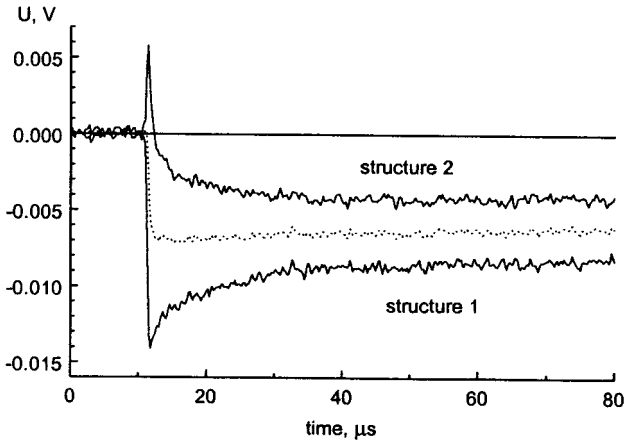

Figure 3. Photovoltage responses of the 100% ZnPQ1 monolayer films deposited in upward (structure 1) and downward (structure 2) directions. The dashed line is the average of the signals.

photoelectric responses were virtually the same as those reported for the chlorophyll *a* samples showing a stepwise formation and a slow decay (the lifetime corresponds to the measured charge relaxation over the input resistance of the amplifier).[11] The intensities and the polarities of the photoelectric responses were sensitive to the external electric field. Therefore, the behavior of the PQ1,2 samples can be explained by a strong intermolecular aggregation between the pyropheophytin moieties and by the migration of photoinduced charges in those aggregates.

The photovoltage responses for the 100% ZnPQ1 samples were more complex (Figure 3). The signals consisted of a fast rise and, at least, of two decay components. One component had an extremely long lifetime and was sensitive to the external electric field. It can be attributed to the charge migration and recombination in the ZnPQ1 aggregates. The other component was relatively short-lived (lifetime 1−10 μs). The polarity sign of this component was controlled by the sample structure and was in agreement with the expected direction of the vectorial PET for the DA molecules organized on the water surface with the quinone moiety located above the pyropheophytin ring. It can be suggested that the short-lived component corresponds to the relaxation of the CS state of individual DA molecules.

The main objective in our LB film development was to prepare samples which would not show the long-lived component but would exhibit structure-controlled signals from the individual DA molecules. Therefore, intermolecular aggregation should be reduced to a minimum. A traditional method to achieve this is to place the DA molecules in a passive lipid matrix.[5−7,20]

3.2. Monolayers of the DA Compounds. The monolayers of the DA compounds were tested in the following series of matrixes: DOPC, Soya PC, EA, SA, SAm, and DPPA. In agreement with the previous studies,[7,26−28] the lipids with unsaturated carbon chains form soft layers and have better miscibility with other molecules compared to the lipids with saturated chains. Matrixes such as DOPC, Soya PC, and EA can prevent the intermolecular aggregation and are hence preferable for the preparation of homogeneous films. The disadvantage of those matrixes is that they cannot be deposited as multilayer films by themselves. In contrast, the lipids with saturated carbon chains form highly ordered stiff layers, which are easy to deposit as a multilayer film, while the nonlipid molecules such as the DA or other dye compounds are pressed out of that structure and form aggregates even at low concentrations.[7] Consequently, our discussion will be limited here to the investigations of the DA molecules incorporated into the soft-matrix monolayers. These monolayers are then incorporated into multilayer structures that are suitable for the photoelectric measurements.

The isotherms of the DA soft-matrix mixtures were close to those of the pure matrix layer, as the relative concentrations of the DA compounds were low (10% or lower). The deposition of the monolayer can be accomplished with almost a unity transfer ratio (typically in 0.9−1.1 range), which in turn, ensures the presence of the matrix on the support. The presence of the DA compounds in the film was controlled by measuring the absorption spectrum of the film. The spectrum should show a distinct absorption band at 410−430 nm (Soret band) and another band at 660−680 nm (Q-band) for samples with a relative concentration greater than 5 mol %. On the basis of this criterion, PQ1 and PQ2 can be deposited successfully in all of the matrixes studied. Stable transfers were achieved for ZnPQ1, but the sample absorptions were 20−40% lower than expected. In contrast, the deposition of ZnPQ2 was almost unsuccessful; weak absorptions were detected, but a stable transfer was not achieved. Therefore, the following consideration is mainly limited to PQ1, PQ2, and ZnPQ1.

It is noteworthy that the deposition of both ZnPQ1 and ZnPQ2 in the rigid matrixes (SA, SAm, or DPPA) was even less successful. Almost no absorption was observed for the ZnPQ2 samples, and the absorption of the ZnPQ1 samples was considerably lower than expected.

The fluorescence properties of the ZnPQ1 monolayer films in DOPC have been described previously.[8] The properties were found to be in good agreement with the model involving the coexistence of two types of conformers, the folded ones and the open ones. The dominating folded conformers undergo fast and efficient ET and have no direct contribution to the observed fluorescence. The fluorescence observed was due to the open conformers and was quenched by the energy transfer to the folded conformers when the relative concentration of the latter exceeded a critical value defined by the Förster radius. In excess of the folded conformers, the energy transfer is a one-step process and the fluorescence decay can be described by the Förster two-dimensional model[29] leading to the equation

$$\mathrm{I}(t) = I_o \exp(-t/\tau_o - \gamma\,(t/\tau_o)^{1/3}) \qquad (1)$$

where I_o and $I(t)$ are the fluorescence intensities just after a delta-pulse excitation and at a time t, respectively, τ_o is the lifetime of the excited state in the absence of the energy acceptors, and γ is a factor determining the efficiency of the energy transfer. The γ factor depends on the mutual orientation of the energy donor and acceptor, and it is proportional to the quencher concentration c (reduced concentration of the folded conformer in the particular case) and to the Förster critical radius R_o. Numeric calculations have been done for a uniform and random distribution of the quencher,[29] and γ can be derived:[8]

$$\gamma = 1.1465 c R_o^2 \qquad (2)$$

For ZnPQ1 in the DOPC matrix, the analysis of the concentration dependence of the γ factor yielded an R_o value of 50 Å, which represents the critical distance of energy transfer in this system.[8]

The fluorescence decays for ZnPQ1 in the Soya PC and EA matrixes were analyzed in the same manner and gave essentially similar results (see Figure 5). We can assume that the folded conformers dominate in the films, since fluorescence of the ZnPQ1 films was at least 10-fold lower compared to that of Zn

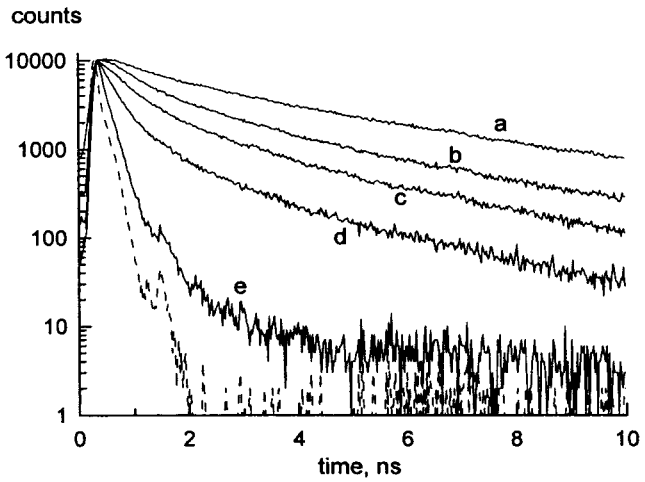

Figure 4. Fluorescence decays of the PQ1 compound in the EA matrix at PQ1 concentrations of (a) 0.6, (b) 1.2, (c) 2.5, (d) 5, and (e) 10 mol %. The instrumental response function is presented by a dashed line.

TABLE 1: Dependence of the Fluorescence Parameters on the Concentration for the Monolayer Films of PQ1 in EA[a]

c, mol %	γ	τ_1, ns	a_1, %	I_{ss}	τ_{av}, ns	I_{PQ1}/I_{PP}
0.6	1.6	7.6	5.6	1.0	2.7	0.32
1.2	3.3	5.8	2.5	0.8	1.2	0.14
2.5	4.7	4.5	1.7	0.4	0.7	0.072
5.0	8.7	2.7	0.66	0.19	0.27	0.059
10.0	18.0	1.6	0.07	0.04	0.066	0.022

[a] Parameters γ, τ_1, and $a_1 = I_e/(I_e + I_F)$ are obtained by fitting of the decay curves by eq 3. I_{ss} is the relative intensity of the steady-state fluorescences compared to a 0.6 mol % sample. τ_{av} is average fluorescence lifetime. I_{PQ1}/I_{PP} is the ratio of the fluorescence intensities of the PQ1 monolayers to the pyropheophytin (reference compound) monolayers.

TABLE 2: Dependence of the Fluorescence Parameters on the Concentration for the Monolayer Films of PQ2 in EA[a]

c, mol %	γ	$\tau_{1,ns}$	a_1, %	I_{ss}	τ_{av}, ns	I_{PQ2}/I_{PP}
0.6	1.7	13	2.7	1.0	2.2	0.27
1.2	2.4	8.6	1.4	1.34	1.6	0.20
2.5	4.1	5.6	0.7	0.79	0.8	0.12
5.0	6.8	3.6	0.22	0.29	0.36	0.075
10.0	13.0	2.4	0.07	0.17	0.12	0.076

[a] For parameters description see Table 1.

pyropheophytin films; hence, the total chromophore concentration can be used in eq 2. There is a clear deviation from the linear dependence on the concentration predicted by eq 2 at low chromophore concentrations. This can be attributed to a distribution of the lifetimes of the open conformers.[8]

The fluorescence properties of the PQ1 and PQ2 compounds in the EA matrix were close to those of ZnPQ1 in DOPC. The fluorescence decay curves for PQ1 at different concentrations are shown in Figure 4. On the quantitative level, the attempts to approximate the decays by the Förster dependence of eq 1 were not as successful as for the ZnPQ1 films. For this reason, the decay curves were fitted in terms of the sum of the Förster and the exponential decay components,

$$I(t) = I_F \exp(-t/\tau_o - \gamma(t/\tau_o)^{1/3}) + I_e \exp(-t/\tau_1) \quad (3)$$

In this case, the statistical χ^2 value was smaller than 1.6. The results of the fittings are summarized in Tables 1 and 2. The exponential decay component showed relatively small amplitudes. At low DA compound concentrations, the component exhibited a lifetime longer than that of the singlet excited state

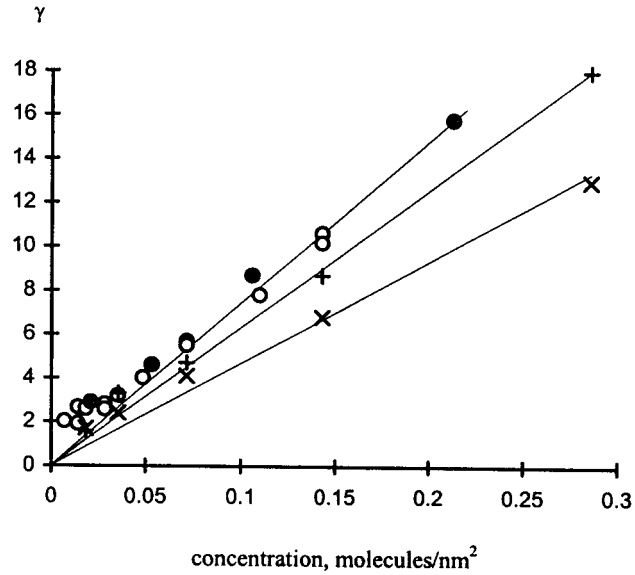

Figure 5. Dependences of the γ factors on the DA concentration for ZnPQ1 in DOPC (○) and in EA (●), and for PQ1 (+) and PQ2 (×) in EA. Straight lines correspond to the critical Förster radii of 50, 42, and 36 Å from top to bottom, according to eq 2.

of pyropheophytin *a* in solutions. For the samples with PQ1 or PQ2 concentration ≥1.2 mol %, the γ factor was almost linearly proportional to the DA molecule concentration, as it was for ZnPQ1 in DOPC. Figure 5 presents the plots of the γ factor vs the DA compound surface concentration for the three types of DA molecules. On the basis of the linear dependencies in Figure 5 and assuming a uniform distribution of the DA dipoles, required by eq 2, the Förster radii can be estimated to be 50 Å for ZnPQ1, 42 Å for PQ1, and 36 Å for PQ2 (see ref 8 for the details of calculations).

The long-lived component in the fluorescence decay curves may be attributed to a possible equilibrium between the singlet excited state (P^SQ) and the CS state,

$$P^sQ \rightleftharpoons P^+Q^- \quad (4)$$

which results in a delayed fluorescence. One can expect that the energy levels of the reactants and products of the ET reaction in the LB films will be close to those in unpolar solvents (e.g., toluene). In a solution with a low dielectric permeability, the ET rate is relatively slow ($k = 0.1-1$ ns^{-1}). This indicates that the energies of the CS state and the singlet excited state are close to each other, thus making the reverse reaction possible. The intensity of the corresponding fluorescence component and, therefore, the efficiency of the reverse ET reaction are low compared to the Förster component (see Tables 1 and 2). This type of process has only a weak effect on the energy transfer occurring in a single step, and hence, the fluorescence decay can be approximated by eq 3 showing a linear dependence of the γ factor on the DA compound concentration. Therefore, we suppose that the model, which takes into account the coexistence of the two types of conformers and the quenching of the fluorescence by energy transfer between the conformers, can be applied to the PQ1 and PQ2 monolayers in the EA matrix.

The long-lived component is essential in the fluorescence decays of PQ1 and PQ2 in the DOPC and Soya PC matrixes. This component is present at all PQ1 or PQ2 concentrations and has a lifetime of 3−4.5 ns. The fast component of the decay curves has a shorter lifetime at higher concentrations of the DA compound. The intensities of the steady-state fluorescence for the PQ1 or PQ2 samples were quenched compared to the

reference samples (quinone-free compounds) by about the same order of magnitude as for the ZnPQ1 samples. The quenching efficiency increased rapidly with the increase in the concentration of the DA compound. Though this type of behavior agrees with the previously discussed model, the fluorescence decay curves cannot be successfully fitted neither to the Förster eq 1 nor to eq 2.

The fluorescence quenching of the PQ1 and PQ2 monolayers in DOPC cannot be explained by the intermolecular aggregation of the phorbin moieties of the DA compound, since the fluorescence time-resolved spectra (1) agreed well with the corresponding fluorescence spectra in toluene solution, (2) were very similar for different concentrations of the DA compound, and (3) were almost time-independent. The proposed explanation is an equilibrium between the singlet excited state and the CS state of the folded conformers. This would allow the energy transfer to occur between the conformers in both directions, from the folded conformers to the open ones and vice versa. The reaction scheme might be as follows:

$$P^s{-}Q \rightleftharpoons P^sQ \rightleftharpoons P^+Q^- \qquad (5)$$

where the left-hand equilibrium represents the intermolecular energy transfer and the right-hand one the intramolecular charge transfer. In addition, the energy transfer between the folded conformers should be taken into account. Thus, the model is approaching a random-walk model involving a multistep energy transfer[30−33] and it is, therefore, difficult to analyze the model quantitatively.

The differences in the fluorescence decays of the DA compounds in the EA and DOPC matrixes can be attributed to different dielectric permeability of the films (mainly defined by the matrix molecules). If the permeability is higher (presumably for EA), the CS state is more stable. Thus, the equilibrium $P^sQ \rightleftharpoons P^+Q^-$ is shifted to P^+Q^-, and the energy transfer is essentially a one-step process ($P^s{-}Q \rightarrow P^sQ$). The behavior of the system is close to that of the Förster type. In contrast, at lower values of the dielectric permeability (DOPC), the P^sQ state is populated enough to make the energy transfer possible in both directions. Under these conditions, the fluorescence decays cannot be described by a simple one-step model.

Unfortunately, we have not been able to prove the above suggestions by electric measurements because of the problems in the multilayer film deposition (see below).

3.3. Deposition of Multilayer Films. The next step in our sample development was the fabrication of multilayer films, suitable for the photoelectric measurements. In these films, the functional layer(s) have to be separated from the electrodes. This can be achieved by the deposition of insulating layers on the electrode below and above the DA compound layer(s). Therefore, the influence of the insulating layers on the fluorescence properties of the DA compounds in soft matrixes was also studied.

It is widely accepted that lipids with saturated carbon chains can serve as insulating layers.[4] The most frequently used lipids are SA, SAm, DPPA, dipalmitoylphosphatidyl choline (DPPC), and other related compounds. For a smooth multilayer deposition of these compounds, a proper subphase, containing certain ions, is needed. Suitable ions are Cd^{2+} and Tb^{3+} for SA, $(UO_2)^{2+}$ for DPPC, Ca^{2+} (or similar bivalent metals) for DPPA, and $(PO_4)^{3-}$ or $(SO_3)^{2-}$ for SAm.[4] The presence of these ions in the water subphase has an influence on the DA layer arrangement and deposition. In addition, the ion−lipid complexes can be transferred into the films and may affect the ET properties of the DA compounds. Consequently, the films of SAm were selected as the first candidates for testing, since they can be deposited from a neutral phosphate subphase; a good alternative for SAm is DPPA, which requires Ca^{2+} ions in the water subphase.

TABLE 3: Deposition of the Multilayer Films Containing Soft Matrix Layers (See Text for Details)

matrix	dep. direction	no. of layers	alternate layer(s)
EA	up	>10	SA, SAm, DPPA
	down	>10	SA, SAm, DPPA
DOLPC	up	<5	SA, DPPA
	down	no transfer	
soya PC	up	10	3 layers of SAm or DPPA
	down	10	3 layers of SAm or DPPA

The films for the electric measurements have to contain DA layers deposited in one direction. However, the deposition of X- and Z-type films is poorly controllable and, hence, it is reasonable to deposit the sample as a Y-type structure with the DA compounds in every second layer (cf. the diagrams shown in section 2 for the complementary structures **1** and **2**). The problem is that the soft lipids cannot be deposited as multilayer structures by themselves, and addition of a small amount of DA molecules did not change the situation. Nevertheless, it was possible to cover the monolayer of the soft matrix by a hard-lipid layer under certain conditions. On this layer, the next soft layer can be deposited. Thus, the problem was solved by alternating the soft-matrix layers, containing the functional DA compounds, with hard-lipid layers.

For the electric measurements, the soft-matrix layers, containing the DA compound, were always deposited in one direction, to give a uniform orientation of the DA molecules. Thus, one or three hard-lipid layers were deposited between the DA layers. Three layers were used if the deposition of the first supporting layer was not successful (transfer ratio less than 0.8). If the third layer had a transfer ratio less than 0.9 or if the deposition of the second soft layer had a transfer ratio less than 0.8, the sample was considered to be unsuccessful.

The results from the testing of different sample structures are summarized in Table 3. We were able to prepare multilayers of the DA compounds in EA in both directions of deposition with a single intermediate layer of SA, DPPA, or SAm. The deposition rate for the EA films was 40 mm/min or faster and for the intermediate layers 20 mm/min, when 0.1 mM $CdCl_2$, $CaCl_2$, or phosphate buffer was used as a subphase. It was possible to prepare a film consisting of as many as 10 layers of Soya PC, alternating each layer by 3 layers of DPPA or SAm. Better films were obtained with DPPA layers. The deposition rate was 40 mm/min for DPPA and 20 mm/min for Soya PC, when 0.1 mM $CaCl_2$ was used as the subphase. By using the DOPC layers alternating with 3 layers of DPPA or SAm, five layers can be deposited, but only for the upstroke direction. The transfer ratio decreases with increasing number of layers, e.g., the fifth layer of DOPC had a transfer ratio of about 0.6.

3.4. Effect of the Bottom Layers on the Structure of the DA Layer. The properties of the DA monolayers deposited on different bottom layers were studied and compared with the monolayers deposited on pure quartz plates. The DA monolayers were always deposited in the upward direction. The transfer ratio for the bottom layers was close to unity. For the DA layers, the transfer ratio varied from 0.8 to 1, depending on the matrix. The absorption intensities of the PQ layers in different matrixes were close to the intensities of the PQ layers without the bottom layers. For ZnPQ1, the monolayer depositions on the bottom layers were less successful. Absorption intensities were significantly reduced in the DOPC matrix independently

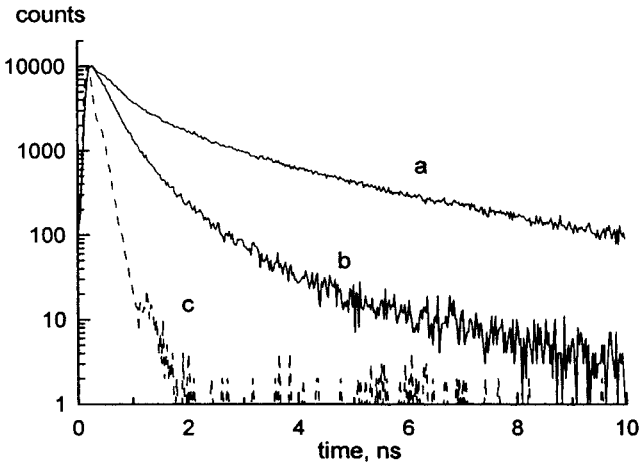

Figure 6. Fluorescence decays for 10 mol % of ZnPQ1 compound in Soya PC matrix deposited (a) onto 10 bottom layers of SAm and (b) directly onto the quartz plate. The instrumental response function is presented by a dashed line.

of the nature of the bottom layers (SA, DPPA, or SAm). Better results were achieved by using Soya PC and EA as the matrixes, although a relative reduction of 20−40% in the absorption of the DA molecules was observed.

The fluorescence decays of the DA compounds deposited directly on quartz plates differed gradually from those deposited on the bottom layers. As an example, Figure 6 presents the decay curves at 670 nm for 10 mol % ZnPQ1 in Soya PC, deposited on (a) SAm bottom layers and (b) on a clean quartz support. The excited state of the DA compound deposited on the quartz plate relaxes faster, and the fluorescence profile fits well to the 2D Förster quenching model, with $\tau_o = 4.7$ ns and $\gamma = 8.2$ in eq 1. Despite the fact that the fluorescence decay of the DA compound deposited on the bottom layers fits badly even to a model with combined exponential and Förster decays (eq 3), it can be approximated with a reasonable $\chi^2 = 1.27$ as a sum of three exponentials with the lifetimes of 60 ± 10 ps, 0.50 ± 0.14 ns, and 2.3 ± 0.1 ns. The three exponentials fitting for curve b in Figure 6 results in the lifetimes of 90 ± 6 ps, 0.36 ± 0.03, and 1.2 ± 0.1 ns, showing smaller difference between the fastest and slowest components than that for curve a. The physical meaning of the three exponentials fitting is not evident. It seems that the homogeneous (random) distribution of the DA molecules in the matrix is disturbed by the supporting bottom layers. There can be clusters of DA molecules with relatively short lifetimes and almost isolated DA molecules with relatively long lifetimes for the excited state. Comparable results were obtained when DPPA and SA bottom layers were used.

For the metal-free PQ compounds, the corresponding analysis is more complex, since the fluorescence decay of the PQ sample does not obey the Förster model of eq 1. On the qualitative level, however, the deposition of the PQ molecules on the hard-lipid bottom layers resulted in the appearance of shorter- and longer-lived components. The fluorescence spectrum of the shorter-lived component was shifted to the red compared to the longer-lived component.

The steady-state fluorescence intensities of the DA compounds deposited on the bottom layers were rather similar to the intensities of the DA compounds deposited on pure quartz plates.

From the viewpoint of PET, the important conformer is the folded one, whose fluorescence is quenched almost totally in the case of ZnPQ1. The only fluorescing conformers are the open ones. Their fluorescence can be quenched by energy

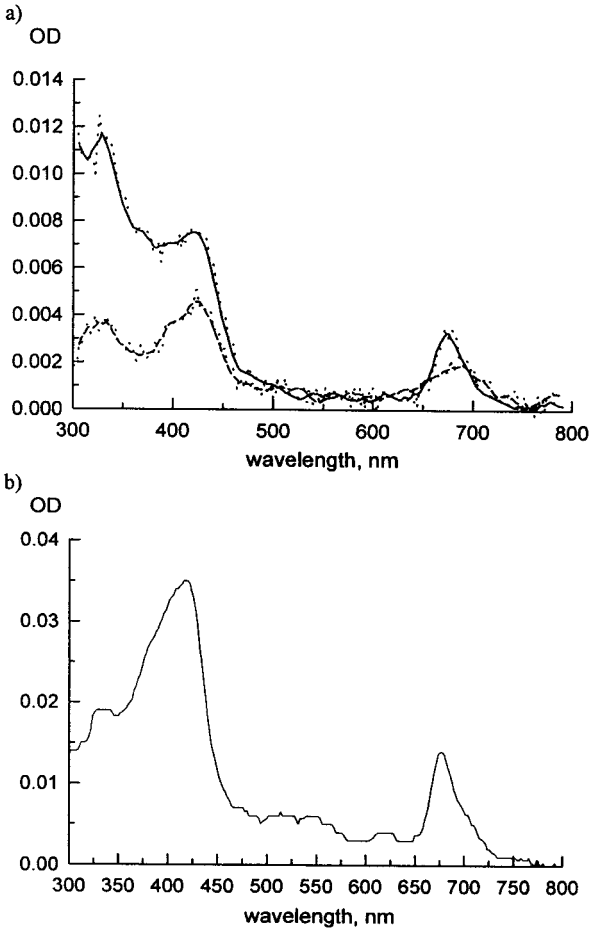

Figure 7. Absorption spectra of samples containing (a) 10 layers of 15 mol % ZnPQ1 in Soya PC matrix each alternated by 3 layers of DPPA and deposited as the structure **1** (dashed line) and the structure **2** (solid line) and (b) 10 layers of 10 mol % PQ1 in EA matrix each alternated by a single SAm layer.

transfer to the folded conformers, and this was used to prove a random distribution of the folded conformers.

The multilayer films were prepared using the method described above. The deposition of ZnPQ1 in the EA matrix was relatively unsuccessful, even when the transfer ratio was about unity. The DA compounds in the multilayer films have shown weak absorption independently of the supporting bottom layers. Rather weak absorptions were observed for the DA compounds in the DOPC matrix as well. The highest absorption for ZnPQ1 was obtained in the Soya PC matrix alternated by DPPA layers, but even in this case the absorption was lower than expected. The transfer ratios for the ZnPQ1−Soya PC layers, when deposited in the upward direction (structure **1**), were somewhat higher than when deposited in the downward direction (structure **2**), but the absorption intensities were higher in the latter case, as shown in Figure 7. The shape of the absorption spectrum for structure **1** exhibits significant broadening of the Q-band, indicating the presence of aggregates of the DA molecules. The fluorescence properties of the multilayer films of structure **1** were quite close to those of the monolayer films deposited on the bottom layers. The fluorescence of the structure **2** samples indicated a lower degree of aggregation. For these samples, the decays were somewhat smoother, but yet no satisfactory fitting could be achieved by applying eq 1 or eq 2.

The absorption intensities of the films incorporating PQ1 or PQ2 were almost proportional to the number of the layers and

the PQ concentration (Figure 7b). Also, some changes in the fluorescence properties were observed, indicating a high degree of aggregation. Basically, the fluorescence properties of the multilayer films containing metal-free DA compounds were close to the properties of the monolayer films deposited on the bottom layers.

In conclusion, the fluorescence and absorption properties of the multilayer samples prepared for the photoelectric measurements indicate higher aggregation tendency for the DA compounds compared to the tendency in the monolayer films deposited on pure quartz plates. The hard-lipid layers may have an effect on the distribution of DA molecules in a soft matrix. The crystal-like structures of the hard lipids may induce more regular packing of the soft-matrix lipids, thus leaving fewer possibilities for the homogeneous distribution of the alien molecules in the matrix.

3.5. Photoelectric Measurements of the DA Films in Lipid Matrixes. All of the multilayer structures were tested by measuring their photoelectric signals. The highest signal intensities were obtained for the ZnPQ1−Soya PC/DPPA multilayer samples. The photovoltage responses in microsecond time domain for the 15% ZnPQ1 samples of structures **1** and **2** are shown in Figure 8. The polarities of the signals are determined by the orientation of the DA molecules in the film. A dominating component in the transient signal is the fast recombination (in less than 0.5 μs) of the CS state. For the 15% ZnPQ1 samples, the contribution of the aggregates of DA molecules to the signal can be found at longer time scales. Also, the relative intensity of the signal, arising from the aggregated DA molecules, is smaller compared to that for the 100% films (see Figure 3). With decreasing concentration of ZnPQ1, the intensity of this signal rapidly decreases. At the concentration of 5 mol %, the photovoltage response consisted almost exclusively of a vectorial intramolecular component. The intensities of the signals for the 5 mol % samples were 20−50% of that for the 15 mol % samples, being in accord with the decrease of the ZnPQ1 concentration.

The deposition of layers consisting of ZnPQ1 in DOPC was less successful, as mentioned above. Nevertheless, signals from the samples containing ZnPQ1−DOPC/SAm or DPPA were detected and can be attributed to the intramolecular ET reaction. The signals indicated a very short lifetime (<20 ns) for the CS state. Unfortunately, only a few layers of these samples could be deposited and hence the intensities of the signals were very weak. Also, since we were able to prepare only samples with structure **1**, we cannot confirm the origin of the photoresponse by comparison with the signals of the complementary structures.

No reliable electric signals, attributable to the vectorial intramolecular ET, were obtained for the ZnPQ1 compound prepared in the EA matrix or for the PQ1 and PQ2 compounds in the tested matrixes.

Two distinct charge-transfer (CT) processes, inter- and intramolecular, should be considered in the discussion of the photoelectric response of the DA compounds. The intermolecular CT takes place between the pyropheophytin moieties of two DA molecules and can be treated as a charge migration along a pyropheophytin aggregate or as a charge hopping between similar sites. This process can be controlled by an external electric field and is independent of the film structure. The intramolecular CT occurs in the same DA dyad molecule, and its direction is determined by the orientation of the dyad. In fact, the electric field must have an influence on the intramolecular ET, as it can introduce some imbalance in the energy (ΔE) of the CS state. The value of ΔE can be estimated from

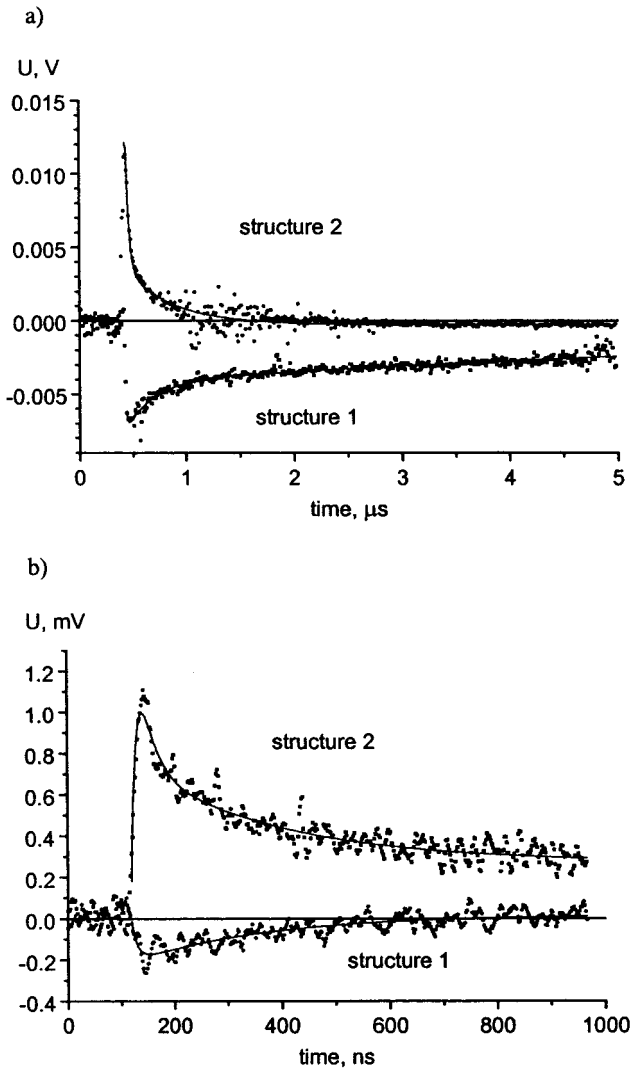

Figure 8. Photovoltage responses of the films of (a) 15 and (b) 5 mol % of ZnPQ1 in Soya PC. The solid lines represent the exponential fittings. For the 15 mol % film, the decay times are 270 ns (43%) and 9.3 μs (57%) for structure **1** and 29 ns (88%) and 450 ns (12%) for structure **2**. For the 5 mol % films, decay times are 190 ns and 26 ns for the structures **1** and **2**, respectively.

the voltage applied to the sample ($U = 1$ V, maximally), the thickness of the film ($L \approx 1000$ Å), and the charge separation distance ($d \approx 4$ Å, the estimated distance between donor and acceptor for the folded conformer of ZnPQ1 in chloroform):

$$\Delta E = Ud/L \approx 0.004 \text{ eV}$$

This value is much less than the thermal energy (kT) and is too small to have any significant influence on the intramolecular ET. That was confirmed in the case of structure **2** (Figure 9), for which neither the intensity nor the lifetime of the fast component depended on the external electric field. The lifetime of the fast component was estimated to be 29 ns, but it is probably shorter and not resolved because the excitation laser pulse duration was roughly 20 ns. At longer delay times, a long-lived component, which can be controlled by the electric field, was detected. It indicates the presence of aggregates in the film, although their relative amount is much lower than that for the 100% film.

The influence of the electric field on the photoresponse from the structure **1** is more complex (Figure 9). The shape of the decay curve is completely different at different polarities of the

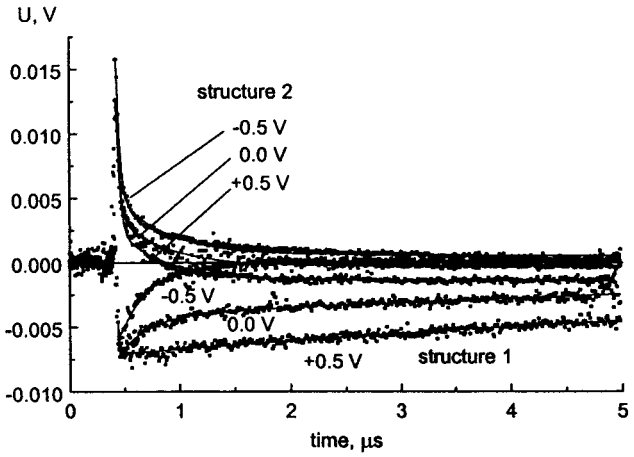

Figure 9. Effect of the external electric field on the photovoltage response of the films containing 15 mol % of ZnPQ1 in Soya PC matrix. The lifetimes, which are independent of the external electric field, are 270 ns and 9.3 μs for the structure **1** and 30 and 450 ns for the structure **2**.

applied voltage. The biexponential fitting resulted in two lifetimes (270 ns and 9.3 μs) for the decay curves shown in Figure 9. The fast component is completely missing when the external voltage was + 0.5 V, but it is dominating at voltage −0.5 V. Most probably the structure **1** samples have a high degree of aggregation compared to the aggregation in the structure **2** samples. This proposal agrees also with the absorption spectra and the fluorescence properties of the samples.

The intra- and intermolecular ET cannot be regarded as independent phenomena. If the charge generated in a DA dyad monomer can be transferred to an aggregate of the DA molecules and can travel inside the aggregate, one can expect the recombination time to depend on the length of the charge migration from the initial donor. Thus, the migration of charge will be controlled by the external electric field. Therefore, the electric field can influence the recombination time without affecting the energy level of the primary CS state. When the electric field is applied in the direction favorable to the primary charge displacement (defined by the sample structure), the recombination time of the separated charges increases.

Comparing the lifetimes of the fast component in cases of DA films with different ZnPQ1 concentrations (Figure 3 and Figure 8, note the time scales), one can find out that the lifetime decreases with decreasing concentration of the DA compound (i.e., with decreasing aggregation). This can also be interpreted in the frame of the present model. A lower degree of the dyad aggregation means a smaller size for the aggregates, and a smaller aggregate size implies a shorter distance for the possible charge displacement from the initial donor. Consequently, the recombination should be faster for the aggregates of smaller size, i.e., at the lower DA dyad concentrations.

It is noteworthy that, in solutions, the recombination time of the CS state is clearly shorter than 10 ns. Therefore, at least for structure **1**, the combination of the intra- and intermolecular ET seems to play an important role in the formation of the long-lived CS state. At low DA dyad concentrations, the photochemically active species can be a dimer, which undergoes a two-step ET resulting in a state like $D^+A\cdots DA^-$.

Conclusions

(1) The recently synthesized DA compounds form a monolayer on the water−air interface, and the monolayer can be transferred onto a solid support as a Langmuir−Blodgett layer.

(2) When incorporated into a matrix of soft lipids (such as Soya phospholipids), the fluorescence properties of the DA compounds indicate light-induced electron transfer for the folded dyad conformer.

(3) For the preparation of multilayer films with uniform orientation of the DA molecules, a method based on an alternating deposition of soft-matrix layers with the DA compound intermitted with layers of hard lipids (such as stearic acid) has been developed.

(4) Light-induced intramolecular electron transfer was observed and studied in multilayer LB films by direct measurements of the Maxwell displacement charge for ZnPQ1 incorporated into the multilayer film.

References and Notes

(1) Wasielewski, M. R. *Chem. Rev.* **1992**, *92*, 435.
(2) Gust, D.; Moore, T. A. *Topics in Current Chemistry*; Springer-Verlag: Berlin Heidelberg, 1991; Vol. 159.
(3) Kuhn, H. *Thin Solid Films* **1989**, *178*, 1.
(4) Roberts, G. *Langmuir−Blodgett Films*; Plenum Press: New York and London, 1990.
(5) Picard, G.; Munger, G.; Leblanc, R. M.; LeSage, R.; Sharma, D.; Siemiarczuk, A.; Bolton, J. R. *Chem. Phys. Lett.* **1986**, *129*, 41.
(6) Tkachenko, N. V.; Grandell, D.; Ikonen, M.; Jutila, A.; Moritz, V.; Lemmetyinen, H. *Photochem. Photobiol.* **1993**, *58*, 284.
(7) Gust, D.; Moore, T. A.; Moore, A. L.; Luttrull, D. K.; DeGraziano, J. M.; Boldt, N. J. *Langmuir* **1991**, *7*, 1483.
(8) Tkachenko, N. V.; Tauber, A. Y.; Hynninen, P. H.; Lemmetyinen, H. *Thin Solid Films* **1996**, *280*, 244.
(9) Ikonen, M.; Sharonov, A.; Tkachenko, N.; Lemmetyinen, H. *Adv. Mater. Opt.Electron.* **1993**, *2*, 115.
(10) Ikonen, M.; Sharonov, A.; Tkachenko, N.; Lemmetyinen, H. *Adv. Mater. Opt. Electron.* **1993**, *2*, 211.
(11) Tkachenko, N. V.; Hynninen, P. H.; Lemmetyinen, H. *Phys. Chem. Lett.* **1996**, *261*, 234.
(12) Desormeaux, A.; Max, J. J.; Leblanc, R. M. *J. Phys. Chem.* **1993**, *97*, 6670.
(13) Jones, R.; Tredgold, R. H.; O'Mullane, J. E. *Photochem. Photobiol.* **1980**, *32*, 223.
(14) Krawczyk, S.; Leblanc, R. M.; Marcotte, L. *J. Chim. Phys.* **1988**, *85*, 1073.
(15) Okamura, E.; Hasegawa, T.; Umemura, J. *Biophys. J.* **1995**, *69*, 1142.
(16) Picard, G.; Aghion, J.; Le Crom, C.; Leblanc, R. M. *Thin Solid Films* **1989**, *180*, 31.
(17) Segui, J.; Hotchandani, S.; Baddou, D.; Leblanc, R. M. *J. Phys. Chem.* **1991**, *95*, 8807.
(18) Tang, C. W.; Albrecht, A. C. *J. Chem. Phys.* **1975**, *62*, 2139.
(19) Tang, C. W.; Albrecht, A. C. *J. Chem. Phys.* **1975**, *63*, 953.
(20) Zelent, B.; Munger, G.; Helluy, A.; Leblanc, R. M. *J. Photochem. Photobiol. A: Chem.* **1991**, *57*, 373.
(21) Tran-Thi, T.-H.; Fournier, T.; Sharonov, A. Yu.; Tkachenko, N.; Lemmetyinen, H.; Grenier, P.; Truong, K.-D.; Houde, D. *Thin Solid Films* **1996**, *273*, 8.
(22) Tauber, A. Y.; Helaja, J.; Tkachenko, N. V.; Lemmetyinen, H.; Kilpeläinen, L.; Hynninen, P. H. In *Photosynthesis: from Light to Biosphere*; Mathis, P., Ed.; Kluwer Academic Publishers: The Netherlands, 1995; Vol. 1, p 815.
(23) Tauber, A. Y.; Kostiainen, R. K.; Hynninen, P. H. *Tetrahedron* **1994**, *50*, 4723.
(24) Tkachenko, N. V.; Tauber, A. Y.; Grandell, D.; Hynninen, P. H.; Lemmetyinen, H. *J. Phys. Chem. A* **1999**, *103*, 3646.
(25) Helaja, J.; Tauber, A. Y.; Kilpeläinen, I.; Hynninen, P. H. *Magn. Reson. Chem.* **1997**, *35*, 619.
(26) Agrawal, M. L.; Chauvet, J.-P.; Patterson, L. K. *J. Phys. Chem.* **1985**, *89*, 2979.
(27) Chauvet, J.-P.; Agrawal, M. L.; Hug, G. L.; Patterson, L. K. *Thin Solid Films* **1985**, *133*, 227.
(28) Chauvet, J.-P.; Agrawa, M.; Patterson, L. K. *J. Phys. Chem.* **1988**, *92*, 4218.
(29) Baumann, J.; Fayer, M. D. *J. Chem. Phys.* **1986**, *85*, 4087.
(30) Grondelle, R. van *Biochim. Biophys. Acta* **1985**, *881*, 147.
(31) Sienicki, K. *J. Chem. Phys.* **1991**, *94*, 617.
(32) Sundstrom, V.; Grondelle, R. van *J. Opt. Soc. Am. B* **1990**, *7*, 1595.
(33) Urquhart, R.; Grieser, F.; Thistlethwaite, P.; Wistus, E.; Almgren, M.; Mukhtar, E. *J. Phys. Chem.* **1992**, *96*, 7808.